THE JOURNAL OF PHYSICAL CHEMISTRY B

Article

pubs.acs.org/JPCB

Energy Migration in Dendritic Oligothiophene-Perylene Bisimides

Jin Zhang,[†,‡] Markus K. R. Fischer,[§] Peter Bäuerle,[§] and Theodore Goodson, III*[,†,‡]

[†]Department of Chemistry and [‡]Department of Macromolecular Science and Engineering, University of Michigan, Ann Arbor, Michigan 48109, United States

[§]Institute of Organic Chemistry II and Advanced Materials, University of Ulm, Albert-Einstein-Allee 11, D-89081 Ulm, Germany

ABSTRACT: A series of novel oligothiophene-perylene bisimide hybrid (DOTPBI) dendrimers up to the second generation (G0, G1, and G2) were investigated. Optical measurements such as nonlinear optical and time-resolved spectroscopy, including two-photon absorption, fluorescence upconversion, and excited state transient absorption were carried out. Results of these measurements revealed the ability of these molecules to undergo intramolecular fluorescence resonance energy transfer (FRET) from the dendritic oligothiophenes (DOT) to the perylene bismide (PBI) moiety. The delocalization length and the photoinduced electron transfer (PET) rate were investigated as a function of dendrimer generation. A fast energy transfer process from the DOT dendron to the PBI core was observed. For the case of the G2 dendrimer, with relatively large thiophene dendrons attached to the bay area of the perylene bisimide, the PBI core is highly twisted and its ability to self-assemble into $\pi-\pi$ stacked aggregates is destroyed. As a result, among the three generations studied, G1, which has the best two-photon cross section and the most efficient energy transfer, is the best light harvesting material.

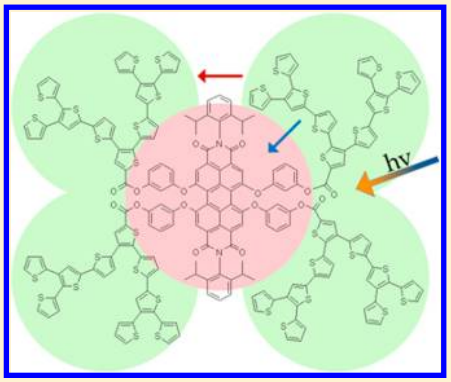

I. INTRODUCTION

Organic conjugated dendrimers are a class of materials with shape-persistent and defined, monodisperse structures that are highly reproducible.[1−3] These macromolecules, which have excellent optical and electrical properties, have been a focus of research for several years, as they have tremendous potential applications in photovoltaic devices,[4,5] light harvesting,[6−9] and organic electronics.[10,11] They have also shown enhanced nonlinear optical (NLO) and two-photon absorption (TPA) properties.[12,13] The geometry of dendrimers suggests a three-dimensional order which might give rise to better overlap for energy transfer. Other structures have demonstrated this property as well. For example, several silsesquioxane (SQ) derivatives with perfect cubic symmetry as well as corner and half partial SQ cages have been synthesized, and their two-photon cross sections have been measured.[14,15] These results imply that the possible demonstration of three-dimensional (3-D) conjugations through the core and the 3-D interaction in the excited state allows for their application as molecular transistors.[14,15] Other geometries of organic conjugated macromolecules have gained tremendous interest and their nonlinear optical properties have been studied. This includes branched chromophore,[16] prion peptide nanostructures,[17] porphyrin macrocycles,[18] and cyclothiophenes.[19] Among the different macromolecules investigated for enhanced NLO and TPA properties, both perylene bisimides and thiophene dendrimers have gained intense interest for their promising potential in organic electronic device application.[20,21]

Perylene bisimide dyes (PBIs) have been developed in the past few years and are now one of the most useful classes of fluorescence materials.[22] PBI dyes exhibit exceptional water solubility, thermal stability, fluorescence intensity, and photochemical stability with high fluorescence quantum yields up to 0.99.[23] Perylene imide derivatives are widely used as the electron acceptor component in the photoinduced energy and electron transfer effects.[24−26] They can be easily functionalized both at the imide and at the bay area to achieve the desired optical and electrochemical properties by various chemical modifications, usually with different substituents. Due to the fully planar π-system shape, PBIs are easily self-assembled into $\pi-\pi$ stacking supramolecular architecture, as aggregates.[27−29] Because of their strong delocalization and efficient charge hopping character, PBIs and other perylene imide derivatives have been suggested as candidates for organic electronics,[30−33] with great potential for applications in light-harvesting systems,[34] solar cells,[35] and field effect transistors.[36] PBIs have served as promising n-type organic semiconductor materials with measured remarkable electron mobilities.[37]

Thiophene dendrimers or dendritic oligothiophenes (DOTs) have also drawn attention because of their versatile applications in organic light emitting diodes (OLEDs),[38,39] light harvesting devices,[40,41] sensor materials,[42] and field-effect transistors (FETs).[43−45] Thiophene dendrimers with a highly branched three-dimensional architecture were first synthesized by Advincula et al.[46] Thiophene-based oligomers have been extensively studied theoretically and experimentally, both for

Special Issue: Paul F. Barbara Memorial Issue

Received: March 22, 2012
Revised: July 26, 2012
Published: July 26, 2012

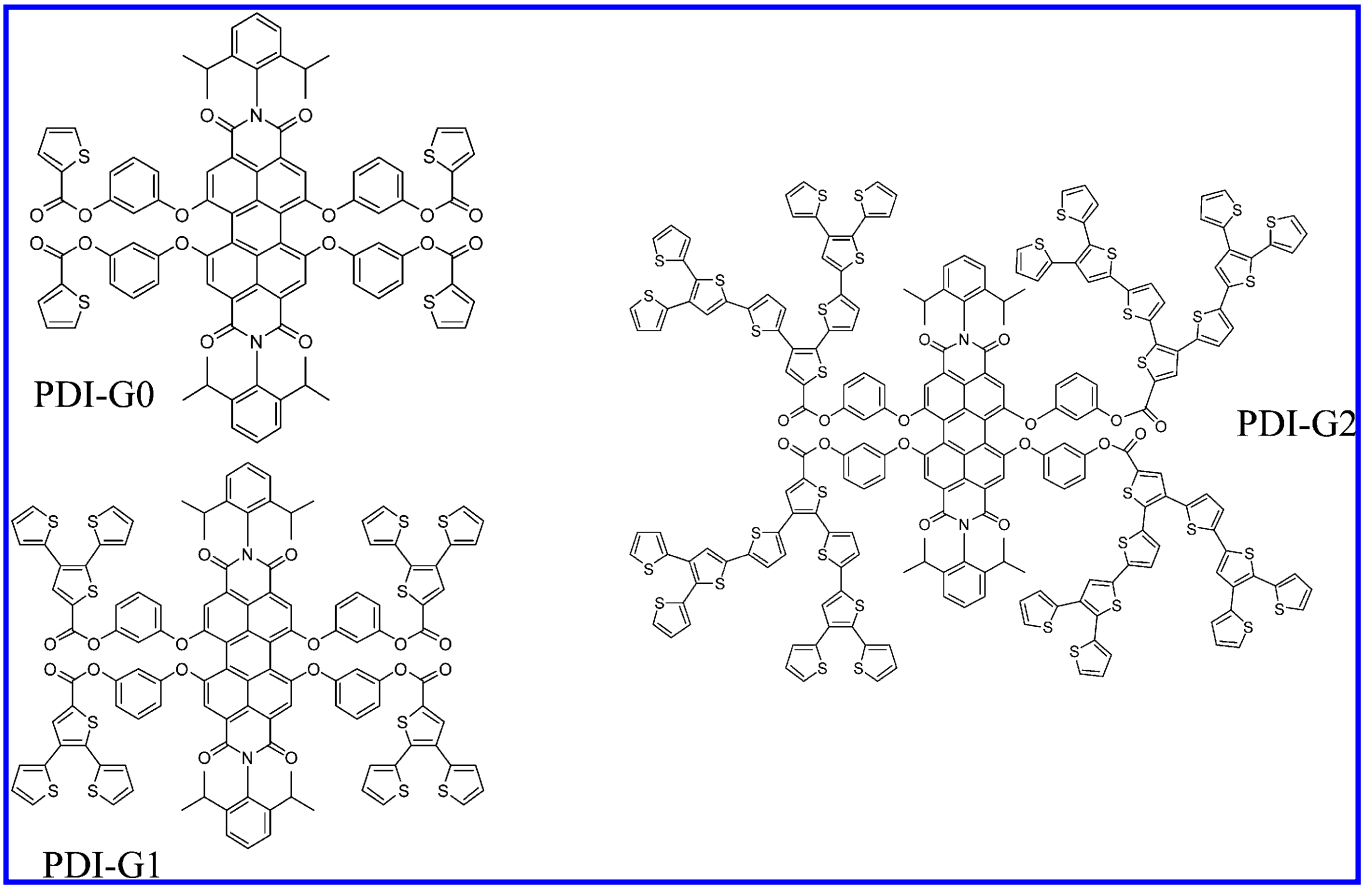

Figure 1. Molecular structure of investigated thiophene dendrimer functionalized perylene imides (PDI-G0, PDI-G1, and PDI-G2).

applications such as light-emitting diodes.[47] Baeuerle et al.[1] developed a new class of large 3-D dendritic oligothiophenes that can be further functionalized at the periphery with other functional groups and easily attached to cores with 3-D geometry and promising optoelectronic properties. Another series of functionalized 3D oligothiophene dendrimers has been synthesized by Baeuerle,[48] and Goodson et al.[21] reported their time-resolved fluorescence up-conversion and transient absorption properties. As these novel semiconducting macromolecules are monodispersed, they offer the significant advantage of reproducibility and unique photochemical properties, which is particularly important for organic electronic devices. The time-resolved spectra of oligothiophenes in solution have also been studied by several groups. Pfeffer et al.[49] first observed the excited state absorption (ESA) and triplet absorption signal of terthiophenes using picosecond photoinduced absorption measurements. Lap et al.[50] reported time dynamics of oligothiophenes using femtosecond time-resolved spectroscopy. Lanzani et al.[51] studied the spectral-dynamic effect of ring rotation of the singlet excited state in oligothiophene derivatives. Unlike PBIs, thiophene dendrimers serve as p-type organic semiconductors.

Recently, a perylene-oligothiophene hybrid as a π-donor$-\pi$-acceptor system has been synthesized and studied by Baeuerle et al.[52] Both DOTs and PBIs are rigid and shape-persistent. As rigid and shape-persistent conjugated dendrimers, these materials represent a novel class of macromolecular materials with defined and monodispersed structures that are highly controllable due to precise synthetic approaches.[45] Because of their three-dimensional structures consisting of a core and shell, these dendrimers possess numerous advantages compared to conventional polymers in offering a number of functionalization schemes. For example, functionalization of the exterior of the dendrimer has been shown to be a promising strategy for sensing applications,[53] while functionalization of the interior of the dendrimer has led to various applications in spectroscopy.[54] It will be very interesting to investigate the energy transfer process of the dendritic thiophene-perylene bisimides as donor-bridge-acceptor type supermolecules with different functional groups as the core and shell separately.

In this work, in order to understand and measure the extent of the energy migration process, the two-photon absorption cross section, fluorescence up-conversion, and excited state dynamics of a thiophene functionalized perylene bisimide system up to the second generation (G0 to G2) have been investigated. The structures of these materials are shown in Figure 1. The TPA cross section in the near IR regions was measured. The fast energy transfer processes from dendron to core and from dendron to dendron are found. The results suggest the ultrafast energy migration in these systems is really efficient. With strong $\pi-\pi$ stacking ability, perylene bisimide is excellent for energy trapping purposes. However, in the higher generation as G2, the tendency of H-aggregation is disrupted due to the highly twisted PBI core. As a result, G2 shows a larger possibility of energy delocalization between the DOT dendrons, lower quantum yield, lower two-photon cross section, and lower energy transfer efficiency than G1. With a smaller size dendron, G1 is the best electron transfer material among those three systems.

dx.doi.org/10.1021/jp302772y | J. Phys. Chem. B 2013, 117, 4204−4215

II. EXPERIMENTAL SECTION

To investigate the optical properties of these oligothiophene-perylene bisimides, several spectroscopic measurements have been carried out, including steady state absorption and emission, two-photon excited fluorescence measurements, fluorescence up-conversion dynamics, and femtosecond transient absorption measurements. All the experiments are carried out in dilute solution with a concentration of $\sim 10^{-6}$ mol/L.

1. Materials. The synthesis of the investigated dendritic oligothiophene-perylene bisimides DOTPBI-G0 (G0), DOTPBI-G1 (G1), and DOTPBI-G2 (G2) has been achieved by Baeuerle et al., and the synthesis procedure was described previously.[55]All the measurements were carried out in dichloromethane (DCM) (Sigma-Aldrich, spectrophotometric grade). All compounds were used as received without any further purification.

2. Steady State Measurements. The absorption spectra of the molecules were measured using an Agilent (Model#8341) spectrophotometer. In order to measure molar extinction coefficients, the original stock solutions were diluted to 10^{-6} M. The fluorescence spectra were acquired using a Spex-Fluorolog-2 spectrofluorimeter. The quantum yields of the molecules were measured using a known procedure.[56] Rhodamine 6G was used as the standard.

3. Two-Photon Excited Fluorescence Measurements. In order to measure the two-photon absorption cross sections, we followed the two-photon excited fluorescence (TPEF) method.[57] The laser used for the study from 700 to 980 nm was a Mai Tai diode-pumped mode-locked Ti:sapphire laser. A 10^{-4} M Coumarin 307 solution in methanol was used as the reference for measuring TPA cross sections at this wavelength range. The 1300 nm beam for the study was produced by an optical parametric oscillator pumped by a Mai Tai diode-pumped mode-locked Ti:sapphire laser. The standard used at this wavelength is style 9 M with a concentration of 10^{-4} M. The laser beam was directed to the sample cell (quartz cuvette, 0.5 cm path length), and the resultant fluorescence was collected in a direction perpendicular to the incident beam. A 1" focal length plano-convex lens was used to direct the collected fluorescence into a monochromator. The output from the monochromator was coupled to a photomultiplier tube (PMT). The photons were converted into counts by a photon counting unit. A logarithmic plot between collected fluorescence photons and input intensity gave a slope of 2, ensuring a quadratic dependence. The intercept enabled us to calculate the two-photon absorption cross sections at different wavelengths. Photo degradation was observed. To solve this problem, the absorption was measured before and after measurements and the average was taken to calculate the concentration.

4. Fluorescence Up-Conversion Spectroscopy and Anisotropy Measurements. The time-resolved fluorescence of the DOTPBI systems was studied using femtosecond up-conversion spectroscopy. The up-conversion system used in our experiments has been previously described.[58,59] We have used both the second harmonic and the third harmonic generation to generate (i) 420 nm, (ii) 377 nm, and (iii) 266 nm, respectively, separately from a mode-locked Ti:sapphire laser for the present investigations. The third harmonic instrument response function (IRF) of this experiment system was determined and reported, and the pulse width is 350 fs.[60] The second harmonic IRF was obtained from the Raman signal of water, and it was found to be around 110 fs.[61] The sample cuvette was made with quartz, 1 mm thick, and held in a rotating holder to avoid possible photodegradation and other accumulative effects. The gate step size in this system is 6.25 fs. Spectral resolution is achieved by dispersing the up-converted light in a monochromator and detecting it by use of a photomultiplier tube (Hamamatsu R1527P). The average excitation power is kept at a level below 3 mW. At these excitation intensities, the fluorescence dynamics were found to be independent of the excitation intensity for all investigated solutions. Polarization of the excitation beam for the anisotropy measurements was controlled using a Berek compensator, and the rotating sample cuvette was 1 mm thick. Horizontally polarized fluorescence emitted from the sample was up-converted in a nonlinear crystal of β-barium borate using a pump beam at 800 nm, which first passed through a variable delay line. Lifetimes were obtained by convoluting the signal with IRF. Spectral resolution was achieved by using a monochromator and PMT. Under these experimental conditions, the investigated dendrimer functionalized perylene imides are quite stable; no photodegradation was observed. Anisotropy measurements were obtained from repeating the fluorescence lifetime measurements with parallel excitation and parallel emission ($I_{\parallel}$) and again with perpendicular excitation and parallel emission ($I_{\perp}$). The total (rotation-free) intensity decay is given by $I(t) = I_{\parallel}(t) + 2I_{\perp}(t)$. Anisotropies as a function of time are then presented as a result of the following relationship, comparing the amplitudes of emission at a given time by $r(t) = (I_{\parallel}(t) - I_{\perp}(t))/(I_{\parallel}(t) + 2I_{\perp}(t))$ for each sample. Use of coumarin 30 as an anisotropy standard provided a G-factor of 0.95. Data fitting and deconvolution at less than 10 ps was done using Surface Xplorer software. Maximum deconvolution time resolution gives a minimum resolution roughly one-sixth of the cross-correlation function, or 30 fs. Data fitting at longer times was performed using Origin 8 software. All emission lifetimes are the result of multi-exponential decay fitting. When contributions to total emission are presented for a given relaxation lifetime as a percentage, the percentage is given as a ratio of the separated and deconvoluted integrations for the decay, weighted by the fitted amplitude for each decay and compared to total emission.

5. Femtosecond Transient Absorption Measurements. Transient absorption was used to carry out the excited state dynamics of the thiophene dendrimers. Briefly, the pump beam was produced by an optical parametric amplifier (OPA-800C). This system contains 1 mJ, 100 fs pulses at 800 nm with a repetition rate of 1 kHz. The output beam was split to generate pump and probe beam pulses with a beam splitter (85 and 15%). The pump beams used in the present investigation were obtained from the fourth harmonic of the signal idler beams and were focused onto a 2 mm quartz cuvette containing the sample. The probe beam was delayed with a computer controlled motion controller and then focused into a sample cuvette sapphire plate to generate a white light continuum. The white light was then overlapped with the pump beam in the sample cuvette, and the change in absorbance for the signal was collected by a charge-coupled device (CCD) detector (Ocean optics). Data acquisition was controlled by specialized software from Ultrafast Systems Inc. The typical power of the probe beam was <0.1 μJ, and that of the pump beam was around $\sim$0.1−0.4 μJ per pulse. Magic angle polarization was maintained between the pump and probe beam using a wave plate. The pulse duration was $\sim$130 fs. The sample was stirred

dx.doi.org/10.1021/jp302772y | J. Phys. Chem. B 2013, 117, 4204−4215

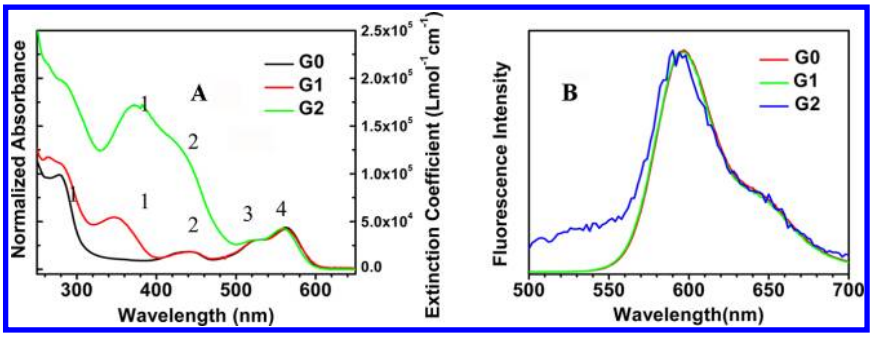

Figure 2. (A) Normalized optical absorption and extinction coefficient and (B) normalized steady-state fluorescence spectra of the investigated derivatives of G0, G1, and G2.

Table 1. Steady-State Properties of Investigated Dendrimer Functionalized Perylene Bisimides

sample	λ_{abs} (nm)	λ_{em} (nm)	Φ_f[a]	E (%)	extinction coefficient (L mol^{-1} cm^{-1}) at different wavelengths	
G0	293(1), 440(2), 525(3), 563(4)	597 645	0.53		N.A.	4.1×10^4 (563 nm)
G1	347(1), 440(2), 525(3), 563(4)	596 645	0.38	69	5.4×10^4 (347 nm)	4.1×10^4 (563 nm)
G2	374(1), 441(2), 525(3), 558(4)	596 644	0.004	46	1.7×10^5 (374 nm)	4.3×10^4 (558 nm)

[a]Quantum yield is measured at a wavelength of 495 nm.

with a rotating magnetic stirrer, and no photo degradation of the sample was observed.

III. RESULTS AND DISCUSSION

1. Steady-State Measurements. The measured optical absorption, fluorescence spectra, and extinction coefficient spectra of the investigated systems dissolved in DCM solvent are shown in Figure 2. A summary of the corresponding steady state properties is shown in Table 1. Comparing these results with the absorption and emission spectra of thiophene dendrons[21] and perylene bisimides,[34,62] the absorption spectra show the features of each moiety in the systems. The result is very clear that the absorption features can be assigned to four regions: below 300 nm, 300−400 nm, 400−500 nm, and 500−600 nm. The absorption features below 300 nm in all of these systems represent the π-to-π^* transition of pure monothiophene units. The absorption features from 300 to 400 nm are the π-to-π^* transition of dendritic thiophene units, and the intensity of these features increases with increasing number of thiophene groups. The absorption region from 400 to 500 nm represents the S0 to S2 electronic transition caused by the dipole moment perpendicular to the long perylene axis. The absorption region from 500 to 600 nm is assigned to the S0 to S1 electronic transition caused by the dipole moment parallel to the long perylene axis. The absorption region from 500 to 600 nm is slightly blue-shifted from 563 nm (for both G0 and G1) to 558 nm (G2). This small change may indicate a small change in the transition dipole moment and less conjugation character possibly as a result of twisting, but the relative sensitivity is not reliable to make a conclusion from steady state absorption alone. Ultrafast techniques or nonlinear optical techniques which are more sensitive can be used to investigate the conformational change of the perylene core.

The extinction coefficient values at different wavelengths are also shown in Table 1. These values in the 300−400 nm region are dramatically increased by increasing the number of thiophenes. As expected, in the 300−400 nm region, the molar extinction coefficient of G2 is about 3 times higher than that of G1, because the number of thiophenes in G2 (36) is also 3 times more than that in G1 (12). The extinction coefficient values between 550 and 600 nm are almost the same.

Due to the energy transfer from the thiophene dendrons to the perylene, the absorption of the perylene in the 400−600 nm region shows about a 13 nm significant red shift in comparison to the (mono) PBIs. The fluorescence emission was excited at several different wavelengths for each compound, which gave very similar emission spectra. In the emission spectra, the peaks at 600 nm with a shoulder at 640 nm are observed as the mirror images of the longest wavelength perylene bisimide absorption bands.[34] G2 has a broad shoulder on the left shoulder side of the emission peak, which is due to the residue of the insufficient energy transfer character from the DOT donor to PBI acceptor.

The quantum yield was measured at a wavelength of 495 nm following a known procedure.[63] Rhodamine 6G was used as a reference (Φ_{fl} = 0.93 in MeOH). The fluorescence quantum yield of PBIs is reported as 0.99.[64] The reported fluorescence quantum yields for pure thiophene dendrons are as low as 0.02.[21] The quantum yield of these three systems decreases significantly with increasing generation. The quantum yield of G2 is 0.004, which is much lower than G0(0.53) and G1(0.38). This is because, when the larger thiophene dendrons are attached, the PBI core of G2 is highly twisted. The relatively bulky thiophene dendrons are highly overlapped and possibly self-quench the emission. As a result, the probability of energy delocalization throughout the entire thiophene dendrons of G2 is highly increased.

The extent of resonant energy transfer (E) is calculated using a known procedure.[64,65] Results are noted in Table 1. In this calculation, the four thiophenes in G0 were neglected, and G0 was used as an acceptor without a donor group. The oligothiophene dendrimers we investigated previously were used as a donor without acceptor.[21] The resulting energy transfer efficiency is as high as 69% for G1 and 46% for G2. The efficiency results indicate the energy transfer process from DOT to PBI is more efficiently founded in the G1 system, and it corresponds well with the quantum yield results. In general, the steady-state absorption and emission results suggest the energy transfer from the PBI to DOT moieties. The energy

dx.doi.org/10.1021/jp302772y | J. Phys. Chem. B 2013, 117, 4204−4215

transfer process in G2 is inefficient. Time-resolved nonlinear optical measurements were carried out to give a better understanding of the transition and mechanism of these systems.

2. Two-Photon Absorption Measurements. The TPA cross section as a function of wavelength has been measured for all the investigated chromophores in the units of Goeppert-Mayer (GM), where 1 GM is 10^{-50} cm^4 s photon^{-1}. It is an indication of charge transfer character and interaction between chromophores. The TPA cross sections of these systems are plotted in Figure 3 with respect to the wavelength in the range

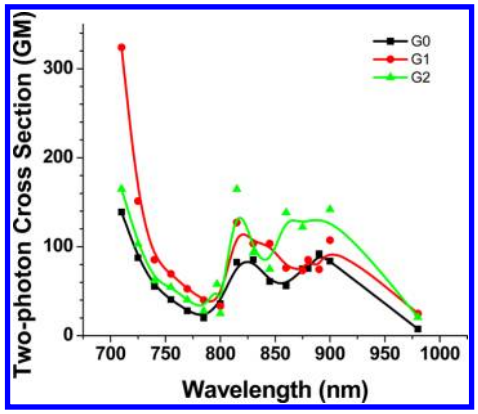

Figure 3. The two-photon absorption cross section for thiophene dendrimer functionalized perylene bisimides.

from 720 to 980 nm. The TPA cross section per molecule and the TPA cross section per thiophene unit at selected wavelengths are listed in Table 2. Previous studies concerning

Table 2. TPA Properties of Silsesquioxane Derivatives

	λ_{ex} = 720 nm		λ_{ex} = 890 nm	
sample	δ (GM)	δ/thiophene (GM)	δ (GM)	δ/thiophene (GM)
G0	129	32	24	6
G1	324	27	43	4
G2	165	5	51	1

the TPA cross section of perylene bisimides derivatives have been reported.[20,66] The TPA cross section of most PBI derivatives is ~100 GM within the scanned wavelength range 840–970 nm. The TPA cross section of DOT dendrons with up to three monothiophenes has been reported.[21] They range from ~6 up to ~150 GM. A super linear relationship between the number of thiophenes and the two-photon cross section was also found. This suggests a substantial increase in cross section with the number of thiophene dendrons, and thus, it is expected that G2 would have a higher TPA cross section than G1. However, this is not the case for our systems noted from Figure 3. When looking at the TPA cross section values between 700 and 780 nm, G1, with less thiophene on each dendron, has a higher TPA cross section than G2. This is due to less charge transfer character caused by the twisted perylene core of G2. The cross section "per branch" in these systems is not enhanced by the additional chromophores in the case of all compounds. In the higher generation, the twisted PBI core destroyed the charge correlation length from the external DOT dendron to the internal core.

3. Fluorescence Upconversion Measurements. Time-resolved fluorescence measurements of the excited and relaxed states are used to investigate the conformational and electronic changes in these systems. Here, we are interested in the variation of fluorescence lifetime and anisotropy decay with excitation of different parts of the macromolecule by using different excitation wavelengths. This is a measurement of the energy transfer process, as well as the extent of the delocalization of the system. The fluorescence decay curves of the chromophores excited at different wavelengths, 420, 266, and 377 nm, are shown in Figures 4, 5, and 6, respectively. The fluorescence detection wavelength is 590 nm. The lifetime results are listed in Table 3.

Shown in Figure 4 is a fluorescence up-conversion decay curve with an excitation at 420 nm. The short time scale fluorescence decay of G0, G1, and G2 with the instrument response function is shown in Figure 4A, B, and C, with the long time scale inserted, respectively. The fluorescence anisotropy is shown in Figure 4D. In the case of G0 and G1, the systems are excited in the absorption band that is the S_0-S_2 electronic transition of perylene, where the dipole moment is perpendicular to the long perylene axis. As reported, the fluorescence lifetime of the singlet excited state of the PDIs is 4.5 ns.[67] Under this excitation, G0 and G1 both show a long-lived lifetime of 4.5 ns. This result corresponds well with the reported fluorescence lifetime of perylene. G2, however, has a much shorter lifetime of 66 ps which is much shorter than the typical fluorescence lifetime of perylene. This discrepancy in the lifetime of G2 is due to the red shift of the dendritic thiophene band which is overlapped with the S_0-S_2 electronic transition of the perylene core. In addition, the excitation is delocalized thoughtout the entire G2 molecule. The rise times after the deconvolution process are 200 fs for G0, 255 fs for G1, and 200 fs for G2. The rise times of G0 and G1 imply the internal conversion of the perylene core. In the case of G2, the existence of fast rise time indicates that the energy has been transferred from the thiophene dendrons to the perylene core.

The fluorescence anisotropy curves are shown in Figure 4D. It should be noted that, under this excitation wavelength, G0 and G1 have an interesting negative anisotropy while G2 shows a positive one. In order to dispel the possibility of aggregation, the steady state absorption and emission results are compared with those of known PBI monomer and π-stacked PBI.[62] Our results follow the trend of PBI monomer very well. Negative anisotropy of perylene with anisotropic rotation has been widely studied.[68] Under the excitation, the absorption and emission transition moments of perylene are nearly perpendicular to each other and the anisotropy at time zero is also reported as −0.14. As a nonspherical and disk-like molecule, perylene has different rotational rates around each axis. The in-plane rotation is much faster than the out-of-plane rotation, because out-of-plane motion requires displacement of solvent molecules. This explains the negative anisotropy of G0 and G1. Unlike planar PBI, G2 behaves as a spherical molecule and it gives rise to the positive sign of the anisotropy with a decay. From the concern of conformational change, it also notes that, with the introduction of a large bay substituent, such as DOT dendrons with 9 thiophene units, the center core in G2 is not as planar or disk-like. This perylene bisimide core in G2 is highly twisted. The degree of the twist is dependent on the apparent overlap parameter of the bay substituents.[69] The dihedral angle is also reported to meet the situated value as 37° with dibromo-substituted PBI. These large dendritic thiophenes at the bay positions can cause core-twisted perylene bisimides. This discrepancy is due not only to the nonplanar geometry but

dx.doi.org/10.1021/jp302772y | J. Phys. Chem. B 2013, 117, 4204–4215

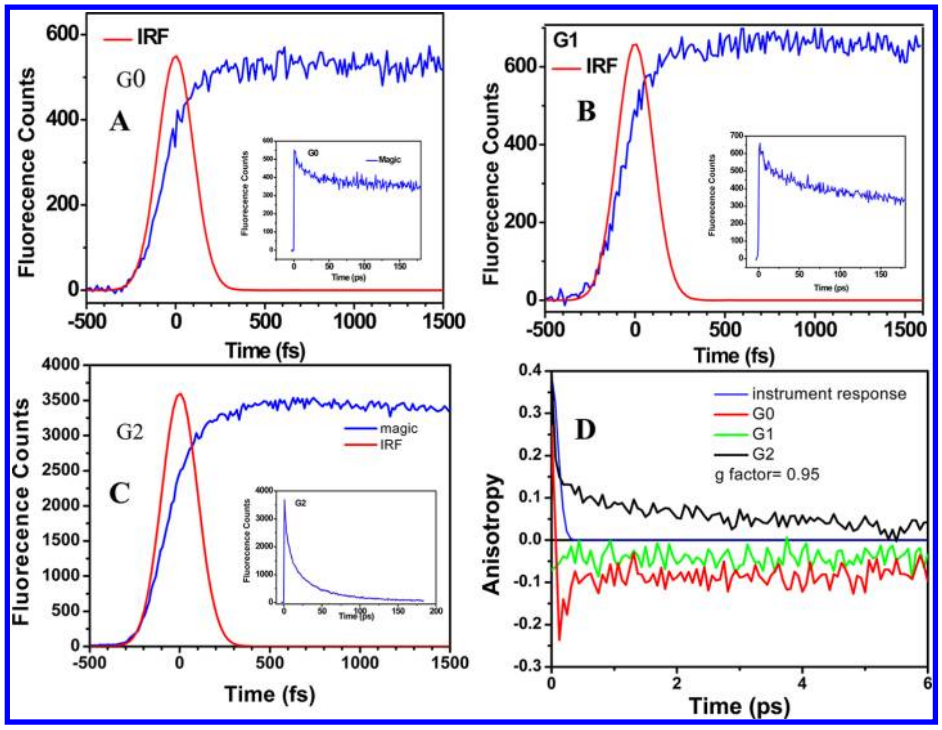

Figure 4. (A–C) Fluorescence and (D) fluorecence anisotropy for the investigated chromphores of different time scale with an excitation at 420 nm.

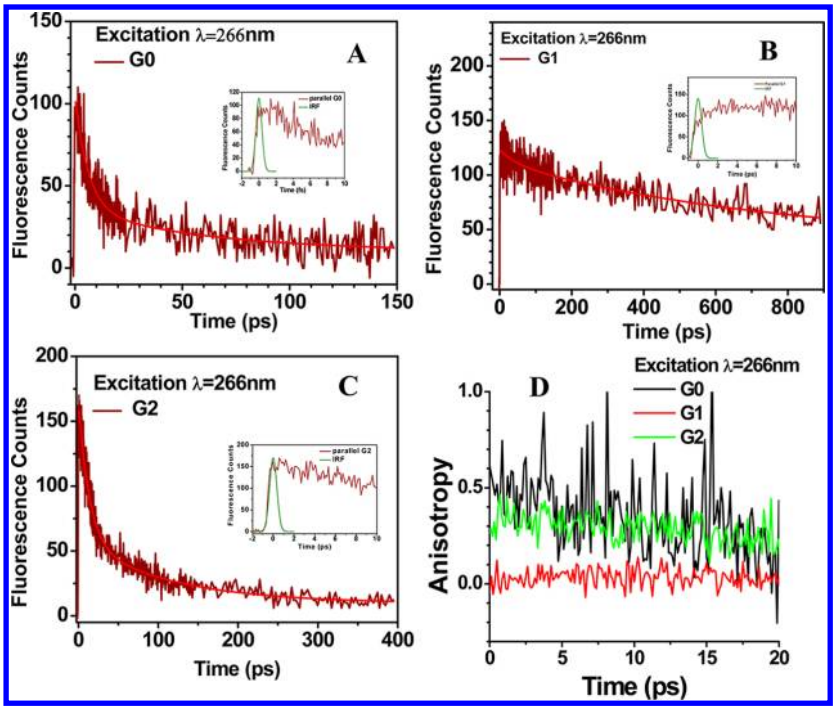

Figure 5. (A–C) Fluorescence and (D) fluorescence anisotropy for the investigated chromphores of different time scale with an excitation of 266 nm.

also to excitation delocalization. By studying the fluorescence up-conversion experiment under this wavelength, we can conclude that both DOT dendrons and PBI core are mainly isolated in the case of G0 and G1, while in the case of G2, it behaves quite different due not only to the interaction between those branches but also the conformational change. Both shortening of lifetime (66 ps) and the different sign of anisotropy decay suggests that, in the case of G2, the excitation is delocalized up to the thiophene dendrons.

Figure 5 shows the fluorescence anisotropy and fluorescence decay curve with an excitation of 266 nm. The long time scale fluorescence decays of G0, G1, and G2 are shown in Figure 5A, B, and C with the short time scale figure inserted, respectively. Under this excitation, the systems are excited in the thiophene absorption band. The lifetimes of G0 and G2 are 61 ps and 115 ps, respectively, while the lifetime of G1 is in nanoseconds which is much longer. As shown in Figure 5B, G1 shows a rise time of 650 fs, while as shown in Figure 5A and C, G0 and G2

dx.doi.org/10.1021/jp302772y | J. Phys. Chem. B 2013, 117, 4204–4215

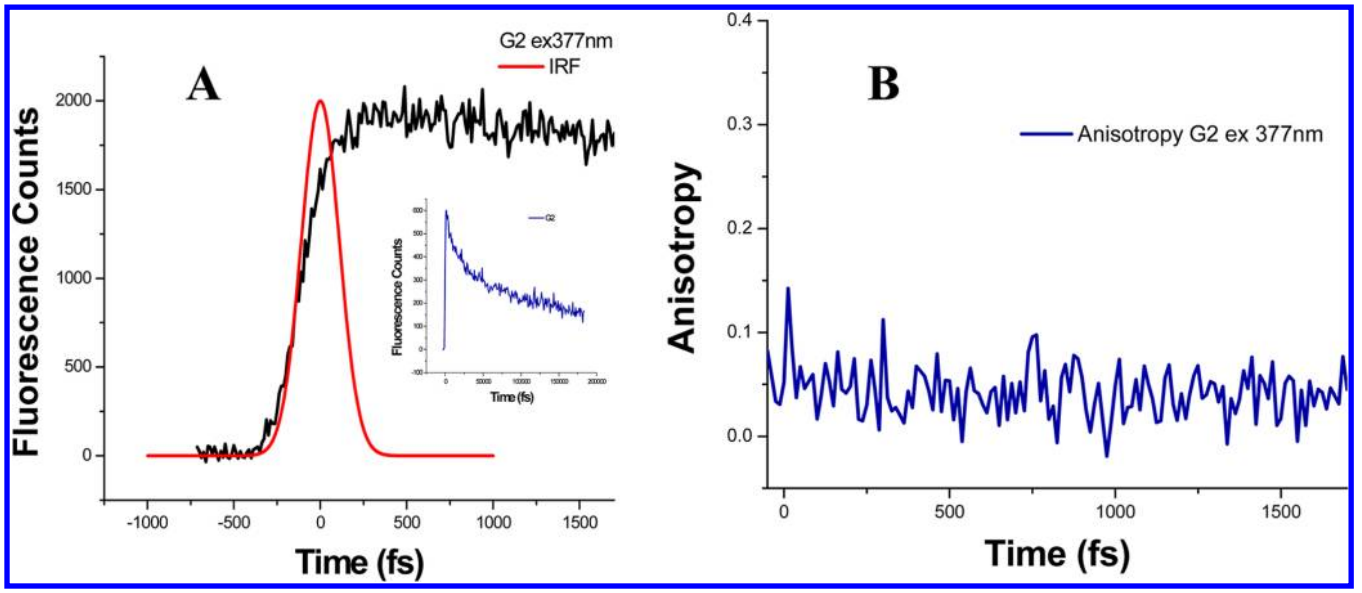

Figure 6. (A) Fluorescence intensity and (B) anisotropy for G2 with an excitation of 377 nm.

Table 3. Fluorescence Lifetime at Different Excitation Wavelengths

	excitation wavelength	lifetime
G0	420 nm	200 fs, 24 ps, 4.5 ns
G1	420 nm	255 fs, 7.4 ps, 95 ps, 4.5 ns
G2	420 nm	200 fs, 13 ps, 66 ps
G2	377 nm	140 fs, 5 ps, 23 ps, 425 ps
G0	266 nm	6.4 ps, 61 ps
G1	266 nm	650 fs, 45 ps, 1 ns
G2	266 nm	14 ps, 115 ps

do not have a rise time. It may because the rise time is faster than the FWHM of the instrument response function. It is also noted that, in Figure 5D, the fluorescence anisotropy of G0 and G2 shows decay from 0.4 to 0, while G1 has a steady anisotropy value of 0. This result indicates that, after the excitation, in the case of G0 and G2, the energy is highly delocalized throughout the entire molecule. In addition, dipole moments of G0 and G2 molecules are more likely randomly orientated at time zero, and then depolarization goes with time within 30 ps. The results of G1, such as extreme long lifetime, localized excitation, and rise time of fluorescence intensity, give the conclusion that the thiophene dendrons and perylene bisimides behave like individual molecules. In the case of G1, the energy is transferred from thiophene to the perylene and then localized at the perylene core which gives the long-lived fluorescence. These results may indicate that G1 is the most suitable one for bulk-heterojunction solar cells among these three materials.

To see the excitation wavelength dependence of the G2 dendrimer, fluorescence up-conversion at an excitation of 377

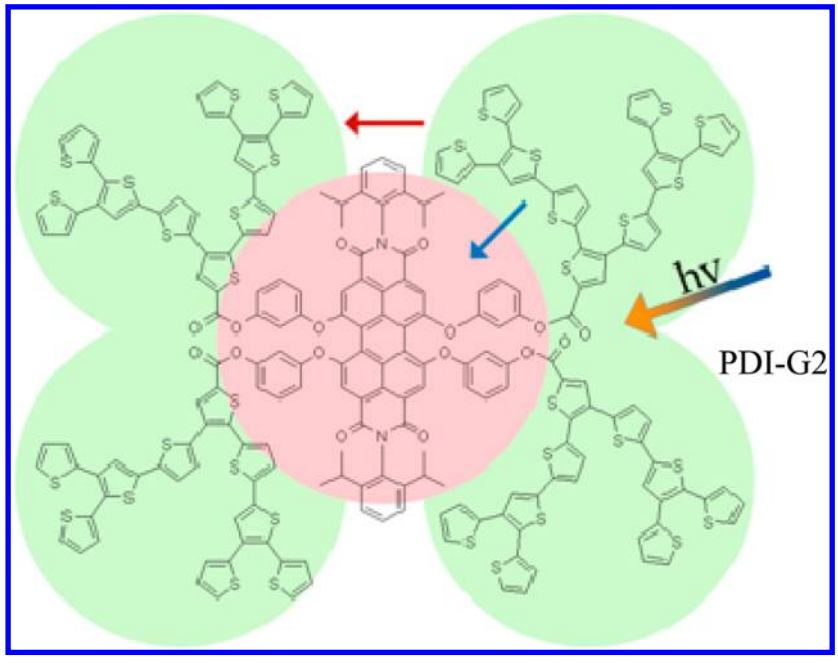

Figure 7. Energy transfer in G2.

dx.doi.org/10.1021/jp302772y | J. Phys. Chem. B 2013, 117, 4204−4215

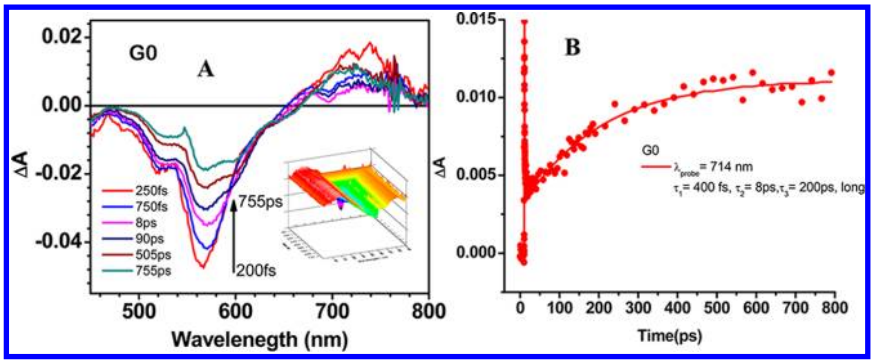

Figure 8. (A)Transient absorption spectra and 3-D spectrum (inserted) of compounds G0 with an excitation of 550 nm. (B) Transient absorption kinetics of G0 at 714 nm.

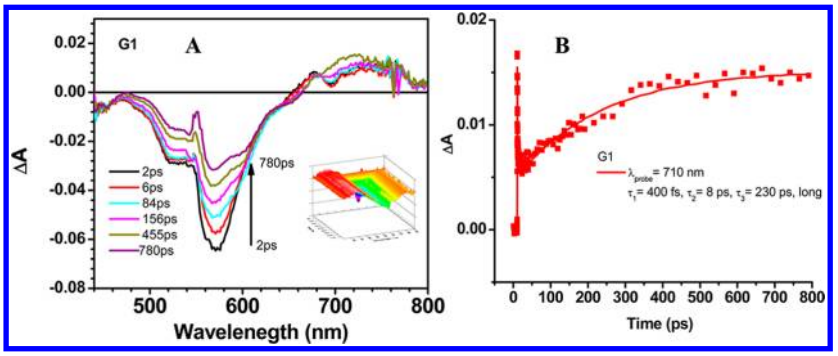

Figure 9. (A) Transient absorption spectra and 3-D spectrum (inserted) of compounds G1 with an excitation of 550 nm. (B) Transient absorption kinetics of G1 at 710 nm.

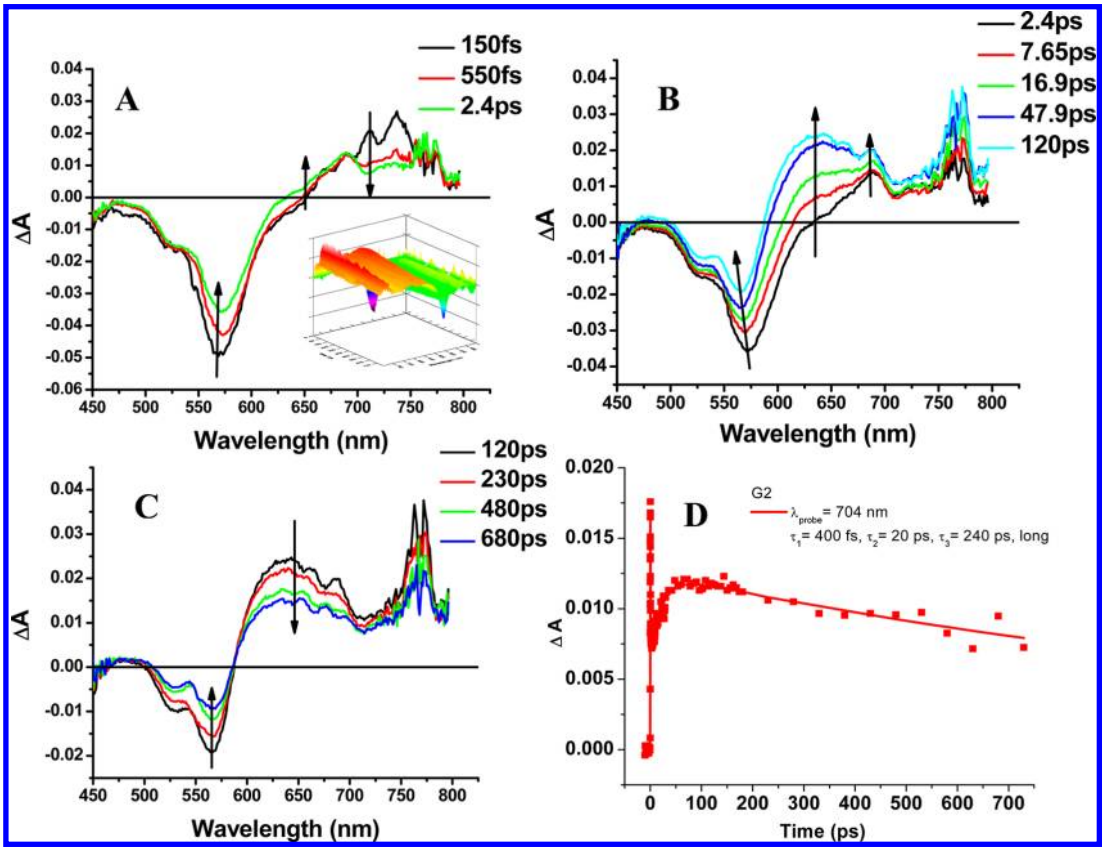

Figure 10. (A–C) Transient absorption spectra of G2 at different times with an excitation of 550 nm. Inserted in part A is a 3-D spectrum of compound G2. (D) Transient absorption kinetics of G2 at 704 nm.

dx.doi.org/10.1021/jp302772y | J. Phys. Chem. B 2013, 117, 4204–4215

nm was also carried out. Shown in Figure 6A and B is the fluorescence decay and anisotropy, respectively. Under this wavelength, we are mainly exciting the thiophene dendrons. It is very interesting to observe that both the rise time (140 fs) and the lifetime (425 ps) of G2 are longer than the case of under excitation of 266 nm. It is observed that the time-zero anisotropy is 0.06 instead of 0.4, in the case of 266 nm excitation. This result suggests the degree of delocalization of G2 depends on the excitation wavelength or the incident photon energy. Numerous similar dynamical processes involving the interaction of excitons with donor and acceptor have been investigated by Barbara et al.[70−76] Figure 7 shows an illustration of the energy transfer process in the G2 system. Excitation energy in G2 can transfer both from DOT to PBI and from DOT to DOT. Charge transfer character is investigated by using ultrafast transient spectroscopy.

4. Time-Resolved Transition Absorption. Femtosecond transient absorption measurements have been carried out in order to understand the fundamental mechanisms of intramolecular excitation. These measurements probe the photoinduced energy and electron transfer processes and may confirm the participation of the electron-transfer process from DOTs to PBIs in dendritic oligothiophene-perylene bisimides. The transient absorption spectra of G0, G1, and G2 in dichloromethane under an excitation at 550 nm are shown in Figures 8, 9, and 10, respectively, with the three-dimensional transient absorption spectra and kinetic dynamics. There are several studies concerning femtosecond transient absorption measurement of PBIs reported in the literature.[34,48,62,77] Wasielewski et al. have studied versatile perylene derivatives using the ultrafast pump−probe transient absorption technique.[78−84] In the previous study, the transient absorption spectra with ground state bleaching bands from 400 to 600 nm and an excited state absorption band from 600 to 800 nm have been obtained.[62] We compared our results with the model PBI[77] (compound PDI0, *N*,*N*′-diphenyl-1,6,7,12-tetrakis[4-(1,1,3,3-tetramethylbutyl) phenoxy] perylene-3,4,9,10-tetracarboxdiimide), in which there is no electron donating group attached to the perylene moiety, and thus no electron transfer process is expected in this molecule. This model PBI exhibited a broad excited state absorption band at the wavelength above 680 nm, as well as a ground state depletion overlapped with the stimulated emission centered at ∼580 nm. The transient absorption of model PBI shows monoexponential decay at the wavelength about 700 nm, with a lifetime around 5 ns. The excited state absorption spectra of G0, G1, and G2 are shown in Figures 8A, 9A, and 10A−C, with 3D excited state absorption spectra inserted. Compared with the model compound, all three dendrimers result in a bleaching of the ground state absorption bands from 500 to 550 nm, accompanied by a strong stimulated emission feature in the 550−600 nm range. This ground state bleaching corresponds well to the singlet-to-singlet transition of the perylene bisimides. As shown in Figures 8A and 9A, both G0 and G1 show excited state absorption bands from 660 to 800 nm. The intensity of the ESA bands of G0 and G1 rises initially and then decays quickly within a few picoseconds. Following this, the ESAs grow steadily with a long-lived lifetime. In the case of G2, which is shown in Figure 10A−C, there is an excited state absorption band in the range 600−800 nm, with blue-shifted ESA compared with G0 and G1. More interestingly, opposite to G0 and G1, the growth of the ESA band of G2 is observed from 2.4 to 120 ps, followed by a decay from 120 to 780 ps. This discrepancy can also be noted from the transient 3D spectra, shown in Figures 8A, 9A, and 10A−C. Compared with the transient absorption features of all three of these dendrimers with different generations, it looks like the G2, which has the most thiophene dendrons, undergoes a significantly different excitation mechanism. This will be discussed later in the section.

The dynamics of the G0 and G1 systems are similar, as shown in Figures 8B and 9B. The kinetics of these two systems can be fitted with a triexponential with 400 fs, 8 ps, around 200 ps and a long time component. The lifetime of the dynamics for each system at different probe wavelength is shown in Table 4.

Table 4. Summary of Lifetimes of G0, G1, and G2

	λ_{pump} = 550 nm			
		τ_1	τ_2	τ_3
G0	λ_{probe} = 716 nm	400 fs	8 ps	200 ps
G1	λ_{probe} = 711 nm	400 fs	8 ps	230 ps
G2	λ_{probe} = 704 nm	400 fs	20 ps	240 ps

The fast component 400 fs can be attributed to the intramolecular excitation energy transfer from the delocalized state to the longest oligothiophene present in the dendron, as found in the thiophene dendrimers.[21] While the other fast component ∼8 ps can be assigned to vibrational/solvent relaxation.[77,85,86] A 200 ps component is related with the absorption and formation of S_1 and the PDI radical anion. The ESA absorption above 680 nm is the PDI S_1-to-S_n absorption[77] and the PDI radical anion absorption.[87−89] Spectra of the ground-state bleaches did not evolve in time, indicating that the ground-state product of the photoinduced event is the same as the initial state. This also proves PDI radical anion formed after excited state excitation occurred. The absorption spectra of thiophene radical cations have been characterized, with steady state absorption maxima at 530 nm.[90] An ESA at this wavelength caused by the formation of the thiophene radical cation, is found overlapping with excited state bleaching.

The transient absorption spectra of G2, shown in Figure 10A−C, give a broad excited state absorption that extends from 650 to 800 nm initially and then shifts to the blue side within 780 ps. This could indicate the charge separated state may be formed from 120 to 780 ps. As a result, the absorption from the charge separated state to the higher excited state happens after accumulation at this state. The longer time scale kinetics trace shows that the stimulated emission recovers with a time scale of 200 ps for the case of G2. The presence of a long-lived transient is observed and overlapped with the simulated emission region. This transient can be assigned to the long-lived triplet−triplet absorption. The recovery kinetics of stimulated emission is much faster than the actual single state lifetime.

G2 shows unique dynamics, which varies from what is found in G0 and G1. Considering G2 contains more thiophene than the other two systems, the transient absorption of thiophene dendrons must be taken into account. Several studies about the dynamics of excited states of oligothiophenes and polythiophene have been carried out using femtosecond transient absorption and time-resolved fluorescence techniques.[51,91] Lanzani et al.[91] have measured the excited state dynamics of oligothiophene and used a two-dimensional model involving vibrational relaxation and torsional relaxation to explain the two main components of the relaxation of the excited state other than the singlet state decay. Similar torsional relaxation has been found in several oligothiophenes and polythio-

dx.doi.org/10.1021/jp302772y | J. Phys. Chem. B 2013, 117, 4204−4215

phenes.[51,87,92−95] Excited state dynamics of oligothiophene dendrons and the coupling between the thiophenes within the dendrimer have also been investigated.[21] The femtosecond transient absorption results have shown the excited state delocalization through the large part of the thiophene dendron and ultrafast energy transfer to the longest oligothiophene in each dendritic unit. A torsional relaxation has also been observed in the final emitting state. A Franck−Condon (FC) state is found for the higher generation of thiophene dendrons, where delocalization happens through a large number of thiophenes in the dendrons. The excited state decays via intersystem crossing to the triplet state. In contrast with the linear oligothiophenes, the excited state dynamics of the thiophene dendrons are actually different due to the presence of a delocalized excited state, an ultrafast energy transfer, and a supplementary torsional relaxation. As shown in Figures 8A, 9A, and 10C, while the amplitudes of the ESA figure of G0 and G1 are increasing steadily after 120 ps, the amplitude of the G2 ESA decays from 120 to 680 ps. This difference can also be easily observed from the kinetics trace curve shown in Figures 8B, 9B, and 10D. The kinetics of G2 at 704 nm is fitted triexponentially with 400 fs, 20 ps, and 240 ps with a long time component. The fast component 400 fs is attributed to the intramolecular excitation energy transfer from the delocalized excited state of the thiophene dendrons to the longest oligothiophene, as found in G0 and G1. And the 240 ps component is related to the electron-transfer rate in G2. From a previous study, it is clearly noted that, as the number of thiophenes increased, the ESA feature in the range 650−800 nm is blue-shifted with increasing ESA intensity. And the excited state delocalization was complete instantly after photoexcitation. The kinetic time components of a series of pure thiophene dendrimers, which have the same structures as thiophene drendrons in the G2 system, were reported with a long time component.[21] The fast component of tens of picoseconds (20 ps) is related to exciton annihilation between chromophores. The kinetic curve of G2 can also be explained by the charge recombination.

The optical properties of macromolecules with multiple chromophores highly depend on the relative orientation and distance between the adjacent chromophores. It has been found out that the zero-order molecular exciton model can be used to predict the coupling of the transition dipole moments by creating two new exciton states.[96] For those chromophores having parallel transition dipole moments, such as perylene bisimide dyes, the transition from the ground state to the higher energy state is fully allowed. As in all three of these systems, the ground state bleaching band around 570 nm is assigned to the transition from the $v = 0$ vibronic level of the ground state to the $v = 1$ vibronic band of the lower exciton state, while the band around 530 nm is assigned to the transition from the $v = 0$ vibronic level of the ground state to the $v = 0$ vibronic level of the upper exciton state. The bleaching bands at 570 nm for G0 and G1 are narrower than that of G2. This suggests that the exciton coupling between adjacent chromophores in G0 and G1 is slightly stronger than that in G2, and the transition moments of G0 and G1 are more parallel than that of G2. As a result, the perylene core is much more twisted in G2 than the case of G0 and G1. There is also a weak excited state absorption change in the transient absorption spectra of the perylene bisimide model at 730 nm.[64] This feature corresponds well with the ESA feature of G0 and G1, which shows less thiophene character than G2. In the case of G2, the different blue shift of the ESA indicates that, as the time goes, there is a certain state accumulating electrons, and after accumulation, these electrons actually go to the higher excited energy state. This blue-shift indicates a strong interaction between the excited PBI and its neighboring thiophene dendrons.

IV. CONCLUSIONS

In conclusion, dendritic oligothiophene-perylene bisimide systems (G0, G1, and G2) have been measured and investigated for their application in light harvesting materials using several nonlinear optical methods. The TPA cross-section of the dendrimer systems is detected in the NIR spectral region. Ultrafast energy transfer and electron transfer from the thiophene dendrons to perylene core has been characterized and compared to model compounds. Femtosecond transient absorption measurements have shown the excited state charge formation of a perylene anion radical at ∼700 nm and the formation of thiophene cation radical near 500 nm. The size of the thiophene dendron has a big influence in the excited-state processes as observed from the time-resolved measurements. For example, in comparing the G0 and G1 dendrimers to the G2 system, one observes an increase in the magnitude of torsional twist as a result of the larger bay substitutes. Thus, the thiophene dendrons overlap strongly. Because of this conformational effect, electrons in G2 are delocalized throughout the entire molecule after excitation. This delocalization process increases the number of pathways of electron transfer from DOTs to the PBI, and thus results in a much faster energy transfer rate, by as much as 8 times. On the other hand, while increasing the size and number of thiophene dendrons, the possibility of exciton annihilation is also increased substantially. Both of these effects have to be taken into account when building up PBI bay area substituted dendritic architectures for their application in the organic photovoltaic area.

AUTHOR INFORMATION

Corresponding Author

*E-mail: tgoodson@umich.edu.

Notes

The authors declare no competing financial interest.

ACKNOWLEDGMENTS

We would like to thank Army Research Office for their financial support of this research.

REFERENCES

(1) Ma, C.-Q.; Fonrodona, M.; Schikora, M. C.; Wienk, M. M.; Janssen, R. A. J.; Baeuerle, P. *Adv. Funct. Mater.* **2008**, *18*, 3323−3331.
(2) Mishra, A.; Ma, C.-Q.; Janssen, R. A. J.; Baeuerle, P. *Chem.—Eur. J.* **2009**, *15*, 13521−13534.
(3) Xia, P. F.; Lu, J.; Kwok, C. H.; Fukutani, K.; Wong, M. S.; Tao, Y. *J. Polym. Sci., Part A: Polym. Chem.* **2009**, *47*, 137−148.
(4) Granstrom, M.; Petrisch, K.; Arias, A. C.; Lux, A.; Anderson, M. R.; Friend, R. H. *Nature* **1998**, *395*, 257−260.
(5) Hagfeldt, A.; Graetzel, M. *Acc. Chem. Res.* **2000**, *33*, 269−277.
(6) Padinger, F.; Rittberger, S. R.; Sariciftci, N. S. *Adv. Funct. Mater.* **2003**, *13*, 85−88.
(7) Jinag, D.-L.; Aida, T. *Nature* **1997**, *388*, 454−456.
(8) Andrews, D. L.; Bradshaw, D. S. *J. Chem. Phys.* **2004**, *121*, 2445−2454.
(9) Donehue, J. E.; Varnavski, O. P.; Chemborski, R.; Lyoda, M.; Goodson, T. *J. Am. Chem. Soc.* **2011**, *133*, 4819−4828.

(10) Forrest, S. R. *Nature* **2004**, *428*, 911−918.
(11) Hoeben, F. J. M.; Jonkheijm, P.; Meijer, E. W.; Schenning, A. *Chem. Rev.* **2005**, *105*, 1491−1546.
(12) Ramakrishna, G.; Bhaskar, A.; Goodson, T., III. *J. Phys. Chem. B* **2006**, *110*, 20872−20878.
(13) Goodson, T., III. *Acc. Chem. Res.* **2005**, *38*, 99−107.
(14) Sulaiman, S.; Bhaskar, A.; Zhang, J.; Ramakrishna, G.; Goodson, T., III; Laine, R. M. *Chem. Mater.* **2008**, *20*, 5563−5573.
(15) Laine, R. M.; Sulaiman, S.; Brick, C.; Roll, M.; Tamaki, R.; Asuncion, M. Z.; Neurock, M.; Filhol, J.-S.; Lee, C.-Y.; Zhang, J.; et al. *J. Am. Chem. Soc.* **2010**, *132*, 3708−3722.
(16) Ramakrishna, G.; Goodson, T. *J. Phys. Chem. A* **2007**, *111*, 993−1000.
(17) Bhaskar, A.; Ramakrishna, G.; Lu, Z.; Twieg, R.; Hale, J. M.; Hagan, D. J.; Van Stryland, E.; Goodson, T. *J. Am. Chem. Soc.* **2006**, *128*, 11840−11849.
(18) Raymond, J. E.; Bhaskar, A.; Goodson, T., III; Makiuchi, N.; Ogawa, K.; Kobuke, Y. *J. Am. Chem. Soc.* **2008**, *130*, 17212−17213.
(19) Bhaskar, A; Ramakrishna, G.; Hagedorn, K.; Varnavski, O.; Mena-Osteritz, E.; Baeuerle, P.; Goodson, T. *J. Phys. Chem. B* **2007**, *111*, 946−954.
(20) Piovesan, E.; Silva, D. L.; Boni, L. D.; Guimaraes, F. E. G.; Misoguti, L.; Zalesny, R.; Bartkowiak., W.; Mendonca, C. R. *Chem. Phys. Lett.* **2009**, *479*, 52−55.
(21) Ramakrishna, G.; Bhaskar, A.; Baeuerle, P.; Goodson, T., III. *J. Phys. Chem. A* **2008**, *112*, 2018−2026.
(22) Neuteboom, E. E.; Meskers, S. C. J.; Van Hal, P. A.; Van Duren, J. K. J.; Meijer, E. W.; Janssen, R. A. J.; Dupin, H.; Pourtois, G.; Cornil, J.; Lazzaroni, R.; et al. *J. Am. Chem. Soc.* **2003**, *125*, 8625−8638.
(23) Grimsdale, A. C.; Muellen, K. *Angew. Chem., Int. Ed.* **2005**, *44*, 5592−5629.
(24) Zhao, Y.; Wasielewski, M. *Tetrahedron Lett.* **1999**, *20*, 7047−7050.
(25) Kelly, R. F.; Shin, W. S.; Rybtchinski, B.; Sinks, L.; Wasielewski, M. *J. Am. Chem. Soc.* **2007**, *129*, 3173−3181.
(26) Giacobbe, E. M.; Mi, Q.; Colvin, M. T.; Cohen, B.; Ramanan, C.; Scott, A. M.; Yeganeh, S.; Marks, T. J.; Rater, M. A.; Wasielewski, M. R. *J. Am. Chem. Soc.* **2009**, *131*, 3700−3712.
(27) Wurthner, F. *Chem. Commun.* **2004**, *14*, 1564−1579.
(28) Fuller, M. J.; Sinks, L. E.; Rybtchinski, B.; Ciaimo, J. M.; Li, X.; Wasielewski, M. *J. Phys. Chem. A* **2005**, *109*, 970−975.
(29) Wasielewski, M. *Acc. Chem. Res.* **2009**, *42*, 1910−1921.
(30) Tauber, M. J.; Kelley, R. F.; Giaimo, J. M.; Rybtchinski, B.; Wasielewski, M. R. *J. Am. Chem. Soc.* **2006**, *128*, 1782−1783.
(31) Newman, C. R.; Frisbie, C. D.; Da Siva, D. A.; Bredas, J. L.; Ewbank, P. C.; Mann, K. R. *Chem. Mater.* **2004**, *16*, 4436−4451.
(32) Ostroverkhova, O.; Cooke, D. G.; Shcherbyna, S.; Egerton, R. F.; Hegmann, F. A.; Tykwinski, R. R.; Anthony, J. E. *Phys. Rev. B: Condens. Matter* **2005**, *71*, 035204-1−035204-6.
(33) You, C.-C.; Hippius, C.; Crune, M.; Wurthner, F. *Chem.—Eur. J.* **2006**, *12*, 7510−7519.
(34) Ahrens, M. J.; Sinks, L. E.; Rybtchinski, N.; Liu, W.; Jones, B. A.; Giaimo, J. M.; Gusev, A. V.; Goshe, A. J.; Tiede, D. M.; Wasielewski, M. T. *J. Am. Chem. Soc.* **2004**, *126*, 8284−8294.
(35) Fortage, J.; Séverace, M.; Houarner-Rassin, C.; Pellegrin, Y.; Blart, E.; Odobel, F. *J. Photochem. Photobiol., A* **2008**, *197*, 156−169.
(36) Schmidt, R.; Oh, J. A. H.; Sun, Y.; Deppisch, M.; Krause, A.-M.; Radacki, K.; Braunschweig, H.; Könemann, M.; Erk, P.; Bao, Z.; et al. *J. Am. Chem. Soc.* **2009**, *131*, 6215−6228.
(37) Tatemichi, S.; Ichikawa, M.; Koyama, T.; Taniguchi, Y. *Appl. Phys. Lett.* **2006**, *89*, 112108−1−112108−3.
(38) Lu, J. P.; Xia, P. F.; Lo, P. K.; Tao, Y.; Wong, M. S. *Chem. Mater.* **2006**, *18*, 6197−6203.
(39) Vaetterlein, C.; Neureiter, H.; Gebauer, W.; Ziegler, B.; Sokolowski, M.; Baeuerle, P.; Umbach, E. *J. Appl. Phys.* **1997**, *82*, 3003−3013.
(40) Chen, T. A.; Rieke, R. D. *J. Am. Chem. Soc.* **1992**, *114*, 10087−10088.
(41) Brabec, C. J.; Sacrittel, N. S.; Hummelen, J. C. *Adv. Funct. Mater.* **2001**, *11*, 15−26.
(42) Harpham, M. R.; Suzer, O.; Ma, C. Q.; Baeuerle, P.; Goodson, T., III. *J. Am. Chem. Soc.* **2009**, *131*, 973−979.
(43) Dodabalapur, A.; Katz, H. E. *Science* **1996**, *272*, 1462.
(44) Sirringhaus, H.; Brown, P. J.; Friend, R. H.; Nielsen, M. M.; Bechgaard, K.; Langeveld-Voss, B. M. W.; Spiering, A. J. H.; Janssen, R. A. J.; Meijer, E. W.; Herwig, P.; et al. *Nature* **1999**, *401*, 685−688.
(45) Schon, J. H; Dodabalapur, A; Bao, Z; Kloc, C.; Schenker, O.; Batlogg, B. *Nature* **2001**, *410*, 189−192.
(46) Xia, C.; Fan, X.; Locklin, J.; Advincula, R. C. *Org. Lett.* **2002**, *4*, 2067−2070.
(47) Garnier, F.; Hajlaoui, R.; Yassar, A.; Srivastava, P. *Science* **1994**, *265*, 1684−1686.
(48) Ma, C.-Q.; Mena-Osteritz, E.; Debaerdemaeker, T.; Wienk, M. M.; Janssen, R. A. J.; Baeuerle, P. *Angew. Chem., Int. Ed.* **2007**, *46*, 1679−1683.
(49) Charra, F.; Fichou, D.; Nunzi, J. M.; Pfeffer, N. *Chem. Phys. Lett.* **1992**, *192*, 566−570.
(50) Lap, D. V.; Grebner, D.; Rentsch, S. *J. Phys. Chem. A* **1997**, *101*, 107−112.
(51) Lanzani, G.; Nisoli, M.; Magni, V.; De Silvestri, S.; Barbarella, G.; Zambianchi, M.; Tubino, R. *Phys. Rev. B* **1995**, *51*, 13770−13773.
(52) Cremer, J.; Bäuerle, P. *J. Mater. Chem.* **2006**, *16*, 874−884.
(53) Trinchi, A.; Muster, T. H. *Supramol. Chem.* **2007**, *19*, 431−445.
(54) Hecht, S. *J. Polym. Sci., Part A: Polym. Chem.* **2003**, *41*, 1047−1058.
(55) Fischer, M. K. R; Kaiser, T. E.; Wuerthner, F.; Baeuerle, P. *J. Mater. Chem.* **2009**, *19*, 1129−1141.
(56) Maciejewski, A.; Steer, R. P. *J. Photochem.* **1986**, *35*, 59−65.
(57) Xu, C.; Webb, W. W. *J. Opt. Soc. Am. B* **1996**, *13*, 481−491.
(58) Varnanski, O.; Yan, X.; Mongin, O.; Blanchard-Desce, M.; Goodson, T., III. *J. Phys. Chem. C* **2007**, *111*, 149−162.
(59) Varnanski, O.; Samuel, I. D. W.; Palsson, L. O.; Beavington, R.; Burn, P. L.; Goodson, T., III. *J. Phys. Chem.* **2002**, *116*, 8893−8903.
(60) Ramakrisha, G.; Goodson, T., III; Rogers-Haley, J. E.; Cooper., T. M.; McLean, D. G.; Urbas, A. *J. Phys. Chem. C* **2009**, *113*, 1060−1066.
(61) Flynn, D. C.; Ramakrishna, G.; Yang, H. B.; Northrop, B. H.; Stang, P. J; Goodson, T., III. *J. Am. Chem. Soc.* **2010**, *132*, 1348−1358.
(62) Giaimo, J. M.; Lockard, J. V.; Sinks, L. E.; Scott, A. M.; Wilson, T. M.; Wasielewski, M. R. *J. Phys. Chem. A* **2008**, *112*, 2322−2330.
(63) Crosby, G. A.; Demas, J. N. *J. Phys. Chem.* **1971**, *75*, 991−1178.
(64) Wu, P.; Brand, L. *Anal. Biochem.* **1994**, *218*, 1−240.
(65) Selvin, P. R. *Methods Enzymol.* **1995**, *246*, 300−334.
(66) Margineanu, A.; Hofkens, J.; Cotlet, M.; Habuchi, S.; Stefan, A.; Qu, J.; Kohl, C.; Klaus Müllen, K.; Jo Vercammen, J.; Yves Engelborghs, Y; et al. *J. Phys. Chem. B* **2004**, *108*, 12242−12251.
(67) Bullock, J. E.; Vagnini, M. T.; Ramanan, C.; Co., D. T.; Wilson, T. M.; Dicke, J. W.; Marks, T. J.; Wasielewski, M. R. *J. Phys. Chem. B* **2010**, *114*, 1782−1802.
(68) Barkely, M. D.; Kowalczyk, A. A.; Brand, L. *J. Chem. Phys.* **1981**, *75*, 3581−3593.
(69) Osswald, P.; Würthner, F. *J. Am. Chem. Soc.* **2007**, *129*, 14319−14326.
(70) Gesquiere, A. J.; Park, S. J.; Barbara, P. F. *J. Am. Chem. Soc.* **2005**, *127*, 9556−9560.
(71) Gesquiere, A. J.; Park, S. J.; Barbara, P. F. *Eur. Polym. J.* **2004**, *40*, 1013−1018.
(72) Tominaga, K.; Kliner, D. A.V.; Johnson, A. E.; Levinger, N. E.; Barbara, P. F. *J. Chem. Phys.* **1993**, *98*, 1228−1243.
(73) Lammi, R.; Barbara, P. F. *Photochem. Photobiol. Sci.* **2005**, *4*, 95−99.
(74) Lee, Y. J.; Zhang, T.; Barbara, P. F. *J. Phys. Chem. B* **2004**, *108*, 5175−5178.
(75) Denny, R. A.; Bagchi, B.; Barbara, P. F. *J. Chem. Phys.* **2001**, *115*, 6058−6071.
(76) Kang, T. J.; Jarzeba, W.; Barbara, P. F. *Chem. Phys.* **1990**, *149*, 81−95.

(77) Flors, C.; Oesterling, I.; Schnitzler, T.; Fron, E.; Schweitzer, G.; Sliwa, M.; Herrmann, A.; Auweraer, M.; van der, C.; de Schryver, F.; Muellen, K.; Hofkens, J. *J. Phys. Chem. C* **2007**, *111*, 4861−4870.
(78) Jones, B. A.; Facchetti, A.; Wasielewski, M. R.; Marks, T. J. *J. Am. Chem. Soc.* **2007**, *129*, 15259−15278.
(79) Odom, S. A; Kelley, R. F.; Ohira, S.; Ensley, T. R.; Huang, C.; Padilha, L. A.; Webster, S.; Coropceanu, V.; Barlow, S.; Hagan, D. J.; et al. *J. Phys. Chem. A* **2009**, *113*, 10826−10832.
(80) Gunderson, V. L.; Krieg, E.; Vagnini, M. T.; Iron, M. A.; Rybtchinski, B.; Wasielewski, M. R. *J. Phys. Chem. B* **2011**, *115*, 7533−7540.
(81) Sinks, L; Fuller, M. J.; Liu, W.; Ahrens, M. J.; Wasielewski, M. R. *Chem. Phys.* **2005**, *319*, 226−234.
(82) Rybtchinski, B.; Sinks, L. E.; Wasielewski, M. R. *J. Phys. Chem. A* **2004**, *108*, 7497−7505.
(83) Ando, S.; Ramanan, C.; Facchetti, A.; Wasielewski, M. R.; Marks, T. J. *J. Mater. Chem.* **2011**, *21*, 19049−19057.
(84) Miller, S. E.; Zhao, Y.; Schaller, R.; Mulloni, V.; Just, E. M.; Johnson, R. C.; Wasielewski, M. R. *Chem. Phys.* **2002**, *275*, 167−183.
(85) Schweitzer, G.; Gronheid, R.; Jordens, S.; Lor, M.; De Belder, G.; Weil, T.; Reuther, E.; Mullen, M.; De, Schryver, F. C. *J. Phys. Chem. A* **2003**, *107*, 3199−3207.
(86) Kaletas, B. K.; Dobrawa, R.; Sautter, A.; Wuerthner, F.; Zimine, M.; De Cola, L.; Williams, R. M. *J. Phys. Chem. A* **2004**, *108*, 1900−1909.
(87) Ford, W.; Hiratsuka, H.; Kamat, P. V. *J. Phys. Chem.* **1989**, *93*, 6692−6696.
(88) Kircher, T.; Lohmannsroben, H. G. *Phys. Chem. Chem. Phys.* **1999**, *1*, 3987−3992.
(89) Wurthner, F.; Sautter, A. *Chem. Commun.* **2000**, *6*, 445−446.
(90) Evans, C. H.; Scaiano, J. C. *J. Am. Chem. Soc.* **1990**, *112*, 2694−2701.
(91) Lanzani, G.; Nisoli, M.; De Silvestri, S.; Tubino, R. *Chem. Phys. Lett.* **1996**, *251*, 339−345.
(92) Lanzani, G.; Nisoli, M.; De Silvestri, S.; Barbarella, G.; Zambianchi, M.; Tubino, R. *Phys. Rev. B* **1996**, *53*, 4453−4457.
(93) Lanzani, G; Nisoli, M; De Silvestri, S.; Tubino, R. *Synth. Met.* **1996**, *76*, 39−41.
(94) Westenhoff, S.; Beenken, W. J. D.; Friend, R. H.; Greenham, N. C.; Yartsev, A.; Sundstrom, V. *Phys. Rev. Lett.* **2006**, *97*, 166804−166808.
(95) Westenhoff, S.; Daniel, G.; Friend, R. H.; Silva, C.; Sundstrom, V.; Yartsev, A. *J. Chem. Phys.* **2005**, *122*, 094903−091911.
(96) Kasha, M.; Rawles, H. R.; El-Bayoumi, M. L. *Pure Appl. Chem.* **1965**, *11*, 371−392.